*Eco. Env. & Cons. 29 (4) : 2023; pp. (1682-1690)*
*Copyright@ EM International*
*ISSN 0971–765X*

**DOI No.: http://doi.org/10.53550/EEC.2023.v29i04.036**

# Projection Modelling Based Geospatial Analysis of Land use Land Cover Change at Hasdeo River Watershed of Chhattisgarh, India

**S.S. Singh and Ankita Singh**

***Department of Forestry, Wildlife & Environmental Sciences***
***Guru Ghasidas University, Bilaspur, Chhattisgarh, India***

(Received 22 April, 2023; Accepted 21 June, 2023)

**ABSTRACT**

The land-use change in the Hasdeo River watershed has been observed with all its sub watersheds. The changing patterns may portend localized impairment to forest and agricultural sub watershed. In this study, Land-use land-cover (LULC) change was modeled using terrset modeling software. The Hasdeo river watershed (geographical extent of 10,396.373 $km^2$) is a part of the Mahanadi River basin in Chhattisgarh, India. Hasdeo River originates from Sonhat (Koriya district, Chhattisgarh) and is submerged into the river Mahanadi. It flows in the stretch of 330 km from north to south direction. This river has eight subwatersheds with rich forest diversity and perennial water resources. IRS-1D & P6 LISS3 images from the years 2000 and 2013 were used to investigate the LULC pattern. This has been used for the prediction of LULC change patterns for the years 2035 and 2050 based on the Markov model. The result of the project LU/LC map for the year 2000-2035 and 2000-2050 show that the dense forest area will decrease by 12.30% and 15.68% respectively. The settlement area will significantly increase by 20.13% (2035) and 34.90% (2050) and will be the dominant land-use type in the watershed. It shows that population pressure will directly affect forest vegetation and agriculture activities. This study will be helpful for the effective sustainability approach for maintaining the proper LULC pattern of land-use change in the watershed. This changing pattern will also influence the farming pattern in the catchment area of the Hasdeo River watershed.

***Key words:*** *Hasdeo Watershed, LULC Classes, Satellite images, Projection model*

## Introduction

In the recent decade, a variety of land-use change models have been developed in the earth system to meet the needs of land management and a better evaluation of the future role of LULC changes. Modeling is a useful tool for predicting alternate future paths, as well as for conducting experiments to test our understanding of essential processes and quantitatively defining them (Veldkamp and Lambin, 2001; Lambin *et al.,* 2000). Satellite-based remote sensing is now widely acknowledged and widely employed to detect LULC changes in a reliable manner.Satellite data are useful, inexpensive, and widely used to create LULC datasets (Singh, 1989; Lu *et al.,* 2014). In the flexible context of GIS, geographic and statistical analysis with modelling are carried out. Satellite imagery is used in GIS technology to monitor land cover types using spectral categorization and Spatio-temporal reflectance to construct linear connections (Masek *et al*., 2008; Tan *et al.,* 2009).

Land use and cover change modelling is currently gaining authentic valuation, and there are numerous modelling programmes available (Pontius and Chen, 2006). In LULC change investigations, only a few previous studies have attempted to combine satellite remote sensing and GIS to qualitative modelling methodologies. The Cellular Automata (CA) Markov, Markov chain is one of the most widely used land use and land cover modelling tools and approaches. The cellular automaton is a type of computer which is used in this evaluation process. The Markov model is a form of spatial transition-based model that may be used to forecast future land development using probabilistic predictions (Rozario *et al.*, 2017; Kokkinos and Maras, 1997). Cellular Automata (CA) has a spatial component (Soe and Le, 2006), and it can change its state based on a rule that links the new state to the previous state and the states of its neighbours (Clarke and Gaydos, 1998). It is used in LULC models that can mimic a variety of land-use scenarios (Thomas and Laurence, 2006).

To assess the quantitative and qualitative character of the LULC change data and to prioritise locations of impairment within a sub-watershed, Markov Chain models are used. It's a descriptive and interrogative technique for quantifying changes in land usage throughout a human-dominated landscape (Muller and Middleton, 1994). This model examines how LULC affects and interacts with natural resource management practises (Wehmann and Liu, 2015; Merem *et al.*, 2011).

This work describes a method for analysing and forecasting LULC changes in the Hasdeo watershed, which is part of the Mahanadi river basin in Chhattisgarh, India, between 2000 and 2050, using satellite remote sensing, GIS, and Markov chain modelling.

## Methodology

### Study Area

The Hasdeo river is a tributary of Mahanadi River in Central India. It is located between $21^0 45'$ North to $23^0 33'$ North latitude and $82^0 00'$ East to $83^0 04'$ East longitude in Chhattisgarh, India. The total length of the river is 333 km. The geographical extent of the Hasdeo river watershed is 10,396.37 $km^2$. The watershed (Fig. 1) is located in the northern topography of Chhattisgarh, India, and is one of the primary watersheds of the Mahanadi river basin. The watershed is geologically characterized by steep, rocky terrain, the presence of Gondwana rocks, and fertile soil, and it spans in most of the area of the Koriya, Korba and Janjgir-Champa districts of Chhattisgarh state. The research area has a cool and warm sub-tropical climate with a good average rainfall of 1254

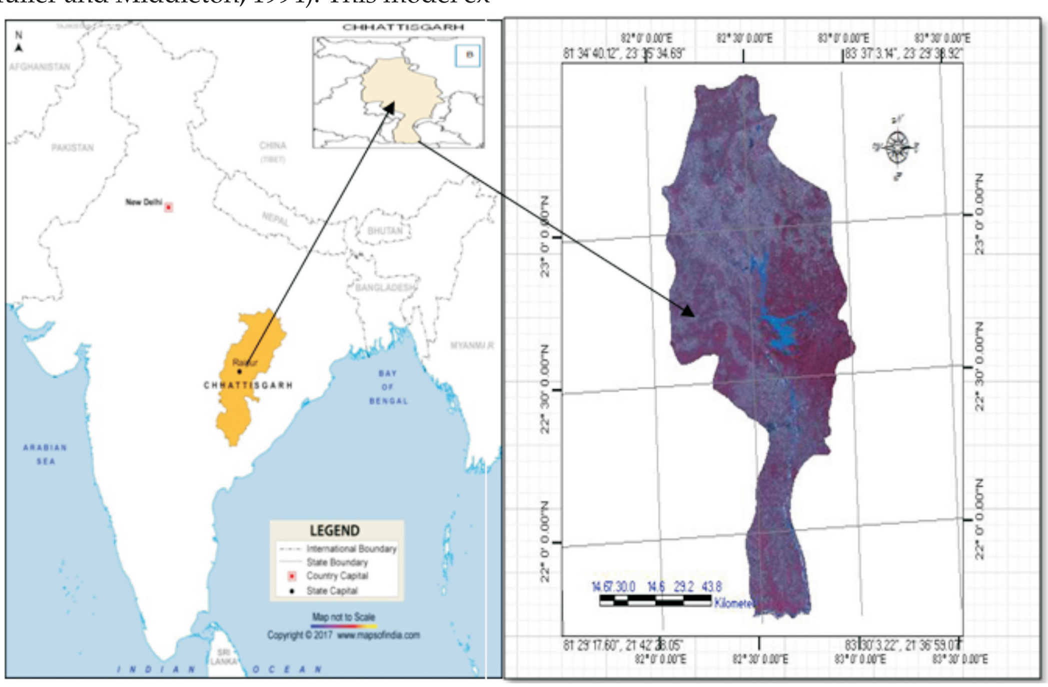


**Fig. 1.** Location of Hasdeo watershed

millimetres. The Hasdeo river (perennial) is the main stream with the Ahiran, Tan, Chornai, Bamhni etc as its tributaries. The topographical conditions in the area is ideal for forest vegetation, irrigation and the production of high-yielding crops. The northern and central part of the watershed is full of tropical dry deciduous type of forest species. *Shorea robusta* is the primary forest tree species found in the area. The other subsidiary species found are *Tectona grandis*, *Terminalia arjuna*, *Terminalia tomentosa*, *Diospyrous melanoxylon*, *Anogeissus latifolia* etc.

## Materials and Methods

The image data products used in this investigation are from the IRS 1-D & P-6 LISS- III (Linear Imaging and Self Scanning) sensor (Indian Remote Sensing). The study employed satellite data from February 2000 and February 2013. The National Remote Sensing Centre (NRSC) Hyderabad, India, provided the satellite data. Table 1 lists the specifications of the satellite data used for change analysis. The flowchart of the research methodology is shown in Fig. 2.

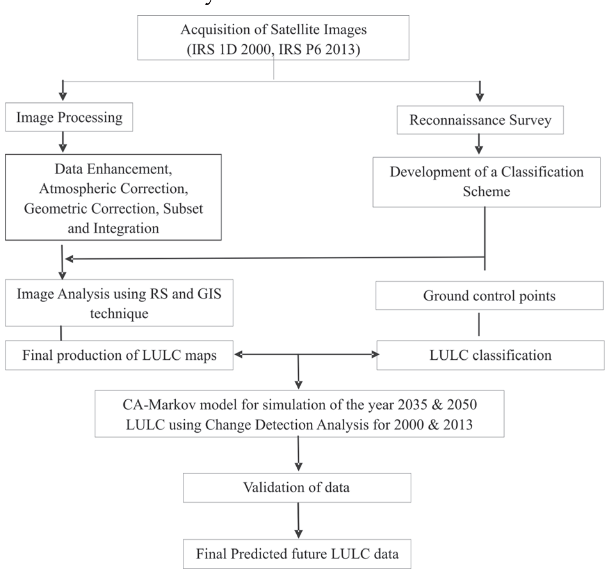


*Source:* Khawaldah, 2016

Fig. 2. Flowchart of the study methodology

### Image Processing

Prior to the identification of change, satellite image pre-processing is critical, with the primary goal of building a more direct link between the gathered data and biophysical processes. Change detection also requires data improvement and radiometric correction, which can lessen the disparities between photos in changing atmospheric circumstances. The two photographs were taken in the same season for this. Using ground control points and the Global Positioning System, all of the sceneries were chosen to be radiometrically and geometrically corrected (GPS). The IRS raw data was delivered in Digital Number (DN) format, which represent reflected radiance for each pixel and this was done using absolute radiometric correction by measuring the spectral reflectance of a reference object in the image. IRS1 D and P6 image raw data were delivered in Digital Number (DN) format, which represent reflected radiance for each pixel at the top of the atmosphere. As a result, it was necessary to use remote sensing software to perform a radiometric correction on the photos in order to convert the DN to reflectance values. This was accomplished by measuring the reference spectral reflectance of the reference object in the image using absolute radiometric correction. To improve the quality of each image, image enhancing techniques such as histogram equalization were used. For the purpose of constructing a series of classed maps, the data of ground control points were altered for each classifier produced by its spectral signature.

**Table 1.** Satellite images and bands were used for the Hasdeo sub-watershed landscape analysis.

| Satellite/Sensor | Year of acquisition | Spectral Band | Resolution |
|---|---|---|---|
| IRS 1D LISS 3 | 2000 | B2: 0.52-0.59 µ<br>B3: 0.62-0.68 µ<br>B4: 0.77-0.86 µ<br>B5: 1.55-1.70 µ | 23.5 m |
| IRS P6 LISS 3 | 2013 | B2: 0.52-0.59 µ<br>B3: 0.62-0.68 µ<br>B4: 0.77-0.86 µ<br>B5: 1.55-1.70 µ | 23.5 m |

Source: National Remote Sensing Centre website (http:// nrsc.gov.in)

### Image analysis and LULC Classification

The hybrid classification technique was used to classify IRS 1D and P6 pictures. Images from 2000 to 2013 were classified using the hybrid classification technique, which combined the findings of unsupervised and supervised classification to get the maximum possible accuracy. Using training areas, a supervised classification method was used. Finally, the unsupervised classification signature was combined with the supervised classification signature. This can assign each pixel in an image to a different land cover class using this method. Using IGIS software, a maximum likelihood technique was used to discover the LULC class types, and then GIS software was used to create the final map, as shown in Fig. 3. This study comprised eight LULC classes in its design. Dense Forest (DF), Open Forest (OF), Waterbody (WB), Riverbed (RB), Fallow Land (FL), Agriculture Land (AL), Settlement (ST) and Mines (M) are the LULC classes . Table 2 lists the descriptions of these classes.

### CA-Markov Model

In GIS, a raster data model is used to describe continuous data over space and to create a specific layer that the TerrSet land change modeller can use. The first technique is to analyse expected LULC based on early and later maps of LULC that have enabled us to obtain transition probability matrix records, which is a probability of each land cover category changing to another category.

Using two LULC in 2000 and 2013 derived from satellite images, the Ca-Markov model was used to predict the change for each class in the years 2035 and 2050, and to apply this model, which is based on the number of a random process, X(t), if the Markov process for any moment of time, t1, t2......tn tn +1, thus, the random process will satisfy the equation:

$Fx(X(t_{n+1})d'' x_{n+1} / X(t_n)=x_n, X(t_{n-1})=x_{n-1}, X(t_1) = Fx(X(t_{n+1}) d'' x_{n+1}) / X(t_n) = x_n)$

When tn is the current time, tn+1 represents some future points, and t1, t2, tn1 represents various points in the past. The future is independent of the past based on current data. To put it another way, the future of a random process is not determined by where it is now or where it was previously. If the Markov chain is expressed by X[k], and the states are x1, x2, x3, then the probability of transitioning from state I to state j in one time instant is; $P_{i,j}$ Pr (X[k+1] = j / X [k] = i)

## Results and Discussion

The correctness of the produced classes (of the classification process) must be tested, hence accuracy assessment is essential. The accuracy is measured using a variety of methods, including overall accuracy and the Kappa coefficient. A total of 18292 pixels were chosen for the IRS-1D LISS3-2000 LULC map, which were subsequently validated against 1:50,000 topographic maps. The overall accuracy of the results is 99.92 percent. Some groups were above 80% in terms of producer and user accuracy, with the exception of open forest, settlement, and barren terrain, which had producer and user accuracy of 55.3 percent, 11.2 percent, and 26 percent respectively. The Kappa agreement index was 99.92 percent. This number indicates that the classification method correctly classified 99.92% of the data.

A total of 32650 pixels were chosen for the IRS-P6-2013 LULC map, which were then validated against 1:50,000 topographic maps. The overall accuracy of the results is 99.75 percent. In terms of user accuracy, waterbody and deep forest classes were above 95 percent and above 85 percent, respectively. The Kappa agreement index was 99.75 percent. This score denotes that the categorization method was successful in avoiding 99.75% of the errors.

**Table 2.** LULC classification classes and description.

| Class | Description |
|---|---|
| Dense forest (DF) | Trees growing very closely together or closed canopy. |
| Open forest (OF) | Trees growing in gaps or open canopy |
| Waterbody (WB) | River, open water, lakes, ponds, and reservoirs |
| Riverbed (RB) | Channel occupied by a river |
| Mines (M) | Land representing coal mines |
| Fallow land (FL) | Land areas of exposed soil and barren area |
| Agriculture land (AL) | Land devoted to agriculture |
| Settlement (ST) | Residential, commercial, industrial, transportation, roads, mixed urban |

Finally, the overall accuracy of more than 90% for the two maps (2000 and 2013) demonstrates that the image processing approach used in this work has proven to be effective in providing compatible LULC data throughout time.

### Detection of LULC

This classification of LULC is done using the USGS Land Cover System classification scheme. The land cover classes were separated into two tiers under the USGS method. To incorporate the LULC classes concentrating on watershed health for the two-time series and build a thematic map to investigate dynamics of distinct LULC classes in the Hasdeo watershed, GIS and remote sensing were employed (Fig. 3). The data showed that between 2000 and 2013, the settlement area and waterbody increased by 1527.39 km$^2$ and 81.81 km$^2$, respectively, indicating that the number of people have increased and this has an influence on agricultural land, dense forest, and fallow land. During the period, the fellow land showed the loss, accounting for 1.04 percent of the total area. Fellow and agricultural land encroachment was evident in the south-western half of the watershed, continuing toward Pali area. Agricultural land, open forest, and dense forest areas, on the other hand, have dropped by 173.43 km$^2$ (1.67 percent), 533.68 km$^2$ (5.13 percent), and 739.81 km$^2$ (7.12 percent) respectively over the same time period.

According to the study, population pressure and

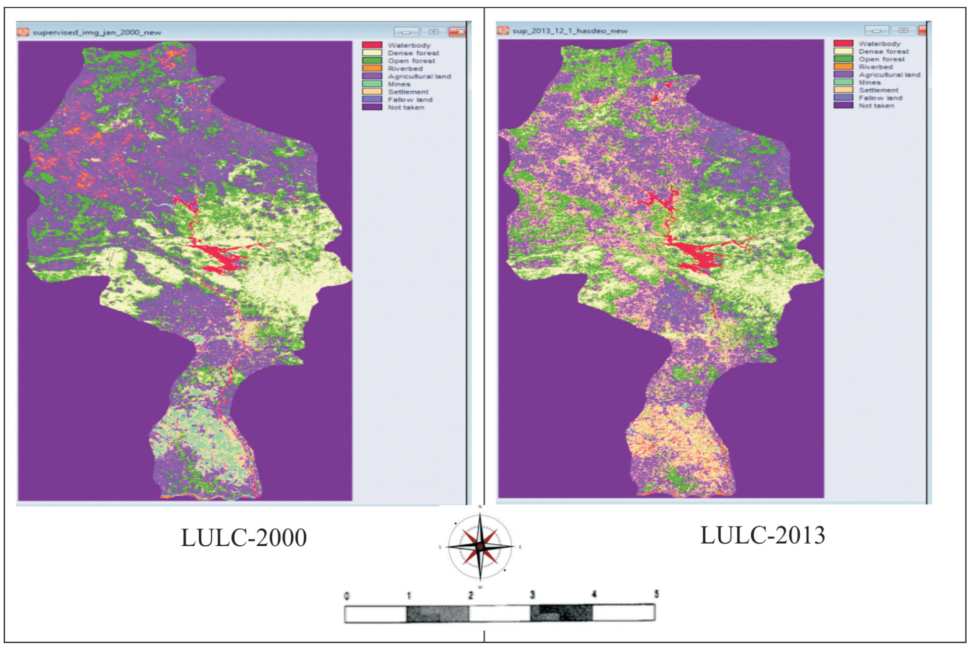


**Fig. 3.** LULC changes during (2000-2013) in Hasdeo watershed

**Table 3.** Area estimation and the overall amount of change in LULC for the study area

| Level 1 | | Level 2 | LULC-2000 | | LULC-2013 | |
|---|---|---|---|---|---|---|
| **Code** | Class name | Class name | Area | | Area | |
| | | | Km$^2$ | % | Km$^2$ | % |
| 1 | OF | Deciduous forest land, Mixed forest land | 2768.45 | 26.63% | 2234.77 | 21.50% |
| 2 | WB | River, Pond, Lake, Streams, Well | 73.81 | 0.71% | 155.62 | 1.50% |
| 3 | DF | Deciduous forest land, Mixed forest land | 2313.11 | 22.25% | 1573.3 | 15.13% |
| 4 | RB | Channels of river | 156.97 | 1.51% | 155.04 | 1.49% |
| 5 | FL | Exposed soil and barren area | 287.96 | 2.77% | 179.89 | 1.73% |
| 6 | AL | Farmlands | 3556.47 | 34.21% | 3383.04 | 32.54% |
| 7 | ST | Residential, commercial, industrial, transportation, roads, mixed urban | 1063.51 | 10.23% | 2590.9 | 24.92% |
| 8 | M | Strip mines, Gravel pits | 176.09 | 1.69% | 123.81 | 1.19% |

settlement probability are constantly exerting pressure on agricultural land, open forest, and dense forest areas. Another decline occurred in the riverbed class, which decreased by 1.93 $km^2$ (0.02 percent) during the same period, contraste to the waterbody class, which gained an additional 81.81 $km^2$ (0.79 percent) due to the good monsoon of 2013. Furthermore, because urban spread generally occurs in a radial fashion around the city centre or in a linear route along highways, a rapid urban sprawl occurred around the Biakunthpur, Korba and Surajpur mining sectors (Sudhira *et al.,* 2004). As a result, Potter *et al.,* (2009) found that the presence of transportation routes inside the study area supported urban sprawl, with city transportation as socially polarised as the city structure itself. The expansion of watershed settlement areas, particularly in town regions, had a severe impact on the local environment. The abundance of water bodies attracts people to stay in the watershed, but water resources are beginning to run out in some mining areas. Farming is the most common activity in the area, with about 80% of the inhabitants involved in some way. Paddy is the main crop, with some legumes and vegetable kinds added for variety. Forest areas in the watershed's southwestern corner have contact tribal inhabitants with the local people. They harvest key forest timber species for personal or social gain. Nonwood forest products such as tendu leaves, sal seed, mahua flower, wild medicinal herbsare not collected informally. The grazing habits of domestic animals have a direct impact on the ability of plants in the forest to regenerate, resulting in a significant loss of forest area over time. As a result, the study employed the Markov model to forecast LULC for the years 2035 and 2050, as well as the future of watershed LULC health and direction, allowing for improved planning in the area.

**Predicting 2035 and 2050 LULC using CA-Markov Model**

The CA-Markov model was used to forecast the 2035 and 2050 LULC based on transition probability matrix records derived from the observed 2000 and 2013 LULC. The main change happened on agricultural land between 2035 and 2050, as per the probability matrix. Agricultural land with settlement areas and open forest, according to fieldwork findings, are transient categories that are subject to larger changes over time.

As illustrated in Figure 3, agricultural land increase is forecast in the south-central part of the existing open forest region in 2035, rather than in the east of the Hasdeo subwatershed. Another 565.33 km2 is expected to be added to the settlement area (to be 30.36 percent of the study area compared to 24.92 percent in 2013). Dense forest and Fallow areas are expected to account for 9.95 percent and 3.05

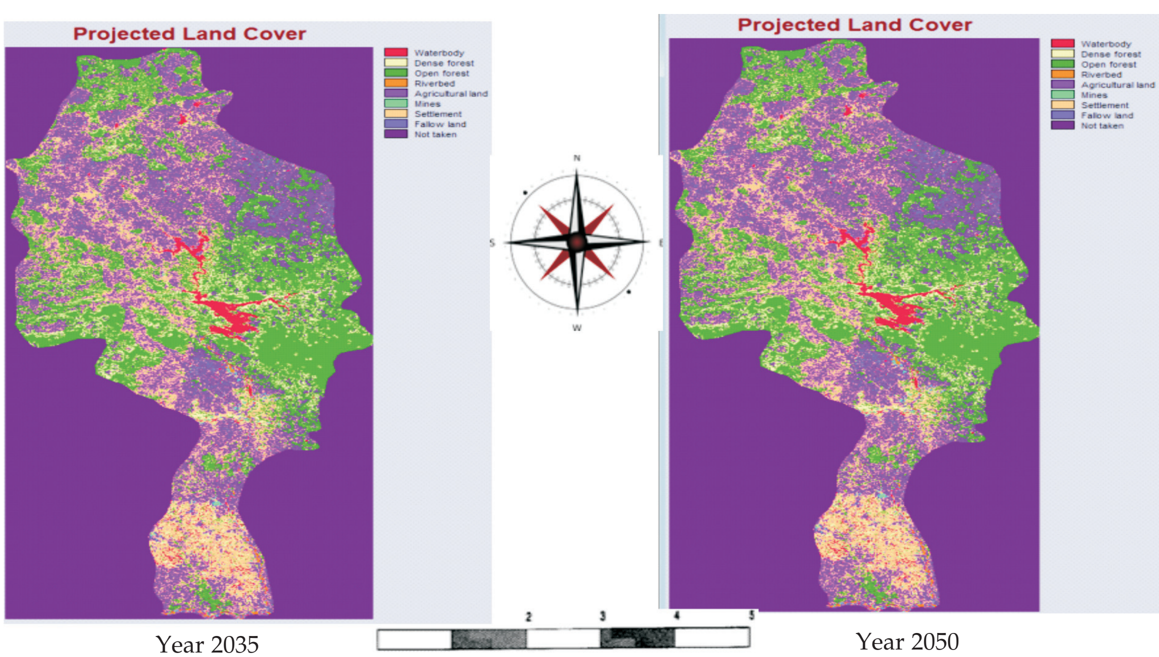


**Fig. 3.** Predicted LULC change from CA-Markov modeling for the years 2035 and 2050

percent of the study area in 2035, respectively, compared to 15.13 percent and 1.73 percent in 2013.

Agriculture land is expected to decrease in the west-central part of the watershed in (2000-2035) and (2000-2050), with 6.08 percent and 9.09 percent, respectively. The dense forest is expected to shrink 12.30 percent during 2000-2035 and 15.68 percent during 2000-2050. The southwestern part of the watershed had the most projected forest decline. However, compared to 25.16 percent (2035), the open forest area is expected to shrink 24.69 percent (2050) (Table 4).

**Validation of CA-Markov Model Results**

The validation of the model's performance is a critical step in determining its capacity to replicate the known data set. In the literature, many goodness-of-fit statistics have been utilised in spatial modelling (Knudsen and Fotheringham, 1986). The performance of the Markov model have been evaluated and its predictions have been validated against a real data set using one main statistical test of goodness-of-fit. $R^2$ (Birkin *et al.*, 2015, Fotheringham, 1986) is a regularly used statistic that is formulated as follows:

$$R^2 = \left[ \frac{\sum_i \sum_j \left(S_{ij} - \bar{S}_o\right)\left(\hat{S}_{ij} - \bar{S}_e\right)}{\left[\sum_i \sum_j \left(S_{ij} - \bar{S}_o\right)^2 * \sum_i \sum_j \left(\hat{S}_{ij} - \bar{S}_e\right)^2\right]^{1/2}} \right]^2$$

Here, $S_o$ represents the mean of the $S_{ij}$'s (observed values) and $S_c$ represents the mean of the $\hat{S}_{ij}$'s (predicted values) and $R^2$ values range between zero and one. The closer the value of $R^2$ is to one the better, since value of one shows an exact correspondence between the observed and predicted values, whilst a zero value reflects correspondence.

Two maps of LULC in the study region for the years 2000 and 2013 were used to calibrate the Markov model in order to construct the 2013 LULC map in the study area using the Markov model (Fig. 4). The Markov-created LULC for 2013 was compared to the observed 2013 LULC of the study area for validation. The model validates the LULC areas as per received data by the user. The comparison of different classes was also based on conversion.

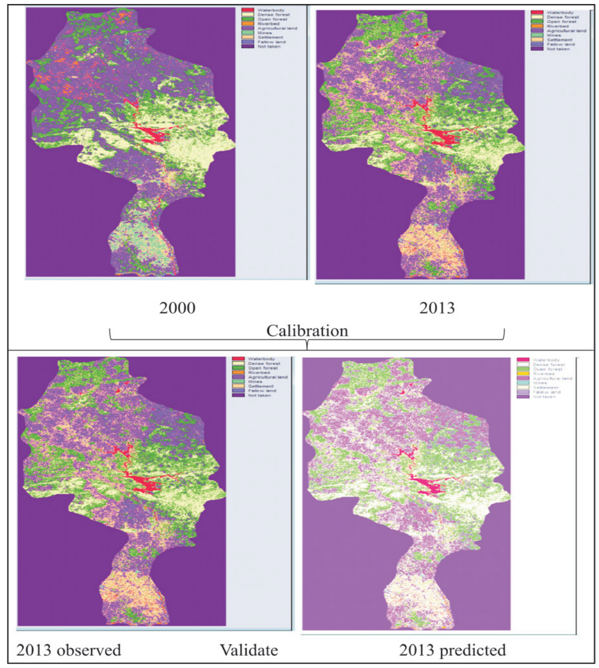


**Fig. 4.** Observed LULC change in 2013 versus the predicted for the same year in Hasdeo watershed

## Conclusion

Not only is it vital to have information about how LULC patterns vary over time for sub-watershed planning, but it is also necessary for better land resource management. This study has demonstrated the value of using RS and GIS techniques to produce accurate LULC maps and change statistics for one of the largest sub-watershed the Hasdeo watershed in Northern Chhattisgarh, which is useful for effectively monitoring settlement, forest area, and agriculture land expansion over time.

The study area's covered dense forest 2313.11 km$^2$ in 2000 and 1573.30 km$^2$ in 2013, or 22.25 percent and 15.13 percent, respectively, as per LULC change detection. However, it is expected to shrink

**Table 4.** Predicted areas of LULC for 2035 and 2050 in the study area

| | LULC classes | OF | WB | DF | RB | FL | AL | ST | M |
|---|---|---|---|---|---|---|---|---|---|
| 2035 | Area in km2 | 2615.74 | 214.16 | 1034.61 | 24.43 | 317.49 | 2924.39 | 3156.23 | 109.32 |
| | Area in %age | 25.16% | 2.06% | 9.95% | 0.23% | 3.05% | 28.13% | 30.36% | 1.05% |
| 2050 | Area in km2 | 2566.77 | 231.83 | 683.02 | 28 | 581.14 | 2611.06 | 3628.1 | 66.45 |
| | Area in %age | 24.69% | 2.23% | 6.57% | 0.27% | 5.59% | 25.11% | 34.90% | 0.64% |

by 1034.61 $km^2$ (9.95%) in the next 22 years, 683.02 $km^2$ (6.57%) in the next 37 years. Agricultural land change detection analysis, on the other hand, shows that agriculture land was 3556.47 $km^2$ (34.21 percent) in 2000, but was reduced to 3383.04 $km^2$ (32.54 percent) in 2013. However, it will be 2924.39 $km^2$ (28.13 percent) and 2611.06 $km^2$ (25.12 percent) in the next 22 and 37 years, respectively. However, the settlement area in the study area was 1063.51 $km^2$ (10.23 percent) in 2000, 2590.90 $km^2$ (24.92 percent) in 2013, and expected to be 3156.23 $km^2$ (30.36 percent) in 2035, and 3628.10 $km^2$ (34.90 percent) in 2050. The statistics show a net decrease in thick forest area in the western, eastern and northern parts watershed. It also suggests that due to the abundant water supply and well-connected highways, the settlement area will be primarily concentrated in the eastern and southern parts.

In the next 37 years (2050), the settlement will also display an increasing pattern, indicating that the population in the area will be high. Because of the abundant work opportunities in the mining and industrial areas, the majority of migratory individuals from the state and other parts of the country will settle in the area. Riverbed, fallow land, and mines areas were converted to habitation and rich water availability between 2000 and 2013.

In the present investigation a GIS-based Markov model have been used to forecast future LULC change in the study area in 2035 and 2050. In 2013, the model was calibrated using satellite pictures from 2000 and 2013 of the study area to anticipate the LULC. The anticipated LULC map in 2013 was then compared to the observed LULC map in 2013. The results of calculating the predicted and observed LULC map of the study are in 2013 revealed that the model performed well in simulating future LULC change within the study area. However, due to the rapid population growth noted above, real LULC class changes in the study area were larger than the expected expansion by the Markov model.

### Study Implications and Future Research

The current study has implications on following three areas can be stated in three areas. First, the findings suggest that dense forest, open forest, and agricultural land declination will occur in several places within the study area in 2035 and 2050, respectively, with an expansion in water body and settlement. In terms of road networks, infrastructure, pond creation, canal formation, agriculture land distribution, and allocating some locations for future watershed management activities, it should be taken into account by forest, agriculture, and water resource planners in their future plans for the Hasdeo watershed. Second, the analysis revealed that settlement and farm land displaced the majority of the forest(dense and open), which may be averted through future regulations or initiatives. Finally, for efficient monitoring of watershed planning and management trends, watershed planners and decision makers should use remote sensing and GIS approaches. As a result, their expectations and predictions of future settlement development and location, forest distribution patterns, and agriculture land utilisation techniques would improve for more sustainable land management.

## Acknowledgement

The author(SSS) wishes to express gratitude to the Ministry of Environment, Forest and Climate Change, New Delhi, India for funding the project. He also express gratitude to the National Remote Sensing Centre in Hyderabad, India, for providing satellite imagery used in the project, as well as the State Forest Department of Chhattisgarh for assistance during field research.

### Conflict of interest

The author declare that they do not have any conflict of interest

## References

Birkin, M., Khawaldah, H., Clarke, M. and Clarke, G. 2015. Applied Spatial Interaction Modelling in Economic Geography: An Example of the Use of Models for Public Sector Planning. In: Karlsson, C., Andersson, M. and Norman, T.,Eds., Handbook of Research Methods and Applications in Economic Geography, Edward Elgar Publishing, Cheltenham, 491-510.

Clarke, K.C. and Gaydos, J. 1998. Loose-coupling a cellularautomaton model and GIS: Long-term urban growth prediction for San Francisco and Washington/Baltimore. *Int. J. Geogr. Inf. Sci.* 12: 699–714.

Congalton, R.G. 1991. A Review of Assessing the Accuracy of Classifications of Remotely Sensed Data. *Remote Sensing of Environment.* 37: 35-46. http://dx.doi.org/10.1016/0034-4257(91)90048-B

Fotheringham, A.S. 1983. A New Set of Spatial Interaction Models: The Theory of Competing Destinations. *Environment and Planning.* A, 15: 15-36.

Kokkinos, E.A. and Maras, A. 1997. A First-Order Stationary Markov Class A Transition Density. *Journal of the Franklin Institute*. 334B: 525-537. https://doi.org/10.1016/S0016-0032(96)00102-0.

Knudsen, D.C. and Fotheringham, A.S. 1986. Matrix Comparison, Goodness-of-Fit, and Spatial Interaction Modelling. *International Regional Science Review*. 10: 127-147. http://dx.doi.org/10.1177/016001768601000203

Lambin, E.F., Rounsevell, M.D.A. and Geist, H.J. 2000. Are Agricultural Land-Use Models Able to Predict Changes in Land-Use Intensity? *Agriculture, Ecosystems & Environment.* 82: 321-331. https://doi.org/10.1016/S0167-8809(00)00235-8.

Lu, D., Li, G. and Moran, E. 2014. Current situation and needs of change detection techniques. *Int. J. Image. Data Fusion*. 5: 13–38.

Masek, J.G., Huang, C., Wolfe, R., Cohen, W., Hall, F., Kutler, J. and Nelson, P. 2008. North American forest disturbance mapped from a decadal Landsat record. *Remote Sens. Environ.* 112: 2914–2926.

Merem, E.C., Yerramilli, S., Twumasi, Y.A., Wesley, J.M., Robinson, B. and Richardson, C. 2011. The applications of gis in the analysis of the impacts of human activities on south Texas watersheds. *Int. J. Environ. Res. Public Health.* 8: 2418–2446.

Muller, M.R. and Middleton, J. 1994. A Markov Model of Land-Use Change Dynamics in the Niagara Region, Ontario, Canada. *Landscape Ecology.* 9: 151-157.

Pontius, Jr. R.G. and Chen, H. 2006. Land Change Modeling with GEOMOD. Clark University, Worcester, USA.

Rozario, Papia F., Oduor, Peter, Kotchman, Larry, Kangas, Michael, 2017. Transition Modeling of Land-Use Dynamics in the Pipestem Creek, North Dakota, USA. *Journal of Geoscience and Environment Protection.* 5: 182-201.

Singh, A. 1989. Review article digital change detection techniques using remotely-sensed data. *Int. J. Remote Sens.* 10: 989–1003.

Soe, W. M. and Le, W. 2006. Multicriteria decision approach for land use and land cover change using Markov chain analysis and a cellular automata approach; *Canadian J. Rem. Sens.* 32: 390–404.

Sudhira, H.S., Ramachandra, T.V. and Jagadish, K.S. 2004. Urban Sprawl: Metrics, Dynamics and Modelling Using GIS. *International Journal of Applied Earth Observation and Geoinformation.* 5: 29-39. http://dx.doi.org/10.1016/j.jag.2003.08.002

Tan, K.C., Lim, H.S., MatJafri, M.Z. and Abdullah, K. 2009. Landsat Data to Evaluate Urban Expansion and Deter- mine Land Use/Land Cover Changes in Penang Island, Malaysia. *Environmental Earth Sciences*. 60: 1509-1521.http://dx.doi.org/10.1007/s12665-009-0286-z.

Thomas, H. and Laurence, H. M. 2006. Modeling and projecting land-use and land-cover changes with a cellular automaton in considering landscape trajectories: An improvement for simulation of plausible future states; *EARSeLeProc.* 5: 63–76.

Veldkamp, A. and Lambin, E.F. 2001. Predicting Land-Use Change. *Agriculture, Ecosystems & Environment.* 85: 1-6.https://doi.org/10.1016/S0167-8809(01)00199-2.

Wehmann, A. and Liu, D. 2015. A Spatial-Temporal Contextual Markovian Kernel Method for Multi-Temporal Land Cover Mapping. *ISPRS Journal of Photogrammetry and Remote Sensing.* 107: 77-89.